



the investigation of the subsurface structures and flows beneath sunspots. The main goal of these studies is to understand the mechanism of formation and stability of sunspots. From the physical point of view, sunspots represent stable, self-organized, magnetic structures in the turbulent convective plasma. Such magnetic self-organization phenomena are of significant interest in physics and astrophysics. In addition, sunspot regions are the primary source of solar disturbances and energetic events.

Previously, the structure of sunspots was studied only from observations of the solar surface. Local helioseismic techniques have provided measurements of variations of travel times and oscillation frequencies associated with the subsurface structure and dynamics of sunspots. These measurements open an opportunity for inferring the subsurface properties of sunspots by inversion of the travel times and frequency shifts. Initially, the local helioseismology studies of sunspots were developed without much theoretical support, using physical intuition and simple models of wave propagation. The criticism of these studies was also based on highly simplified models and arguments. But, recently, substantial progress has been made in developing realistic MHD simulations of dynamics of the turbulent magnetized plasma. Creating a synergy of the local-helioseismology measurements and the simulations is the most recent development in this field, which undoubtedly will lead to new understanding of the sunspot phenomenon.

The inversion (tomographic) procedures of seismology and helioseismology are well-developed, particularly, when the inverse problem is reduced to the solution of integral equations relating variations of the oscillation frequencies and travel times to perturbations of interior properties. However, in the case of sunspots these relationships have not been well-established, and thus the interpretation of helioseismic measurements and inversion results remains uncertain.

The main reasons for the helioseismic uncertainties arise from a complex interaction of solar oscillations with strong magnetic fields of sunspots, non-uniform distribution of wave sources in the sunspot areas, and uncertainties of the helioseismic measurement procedures. The initial inferences have been made by using relatively simple physical relations derived from a ray-path approximation or a first Born approximation. These results caused a significant interest and discussions. With the rapid progress of supercomputing, an important role is being played by direct MHD numerical simulations, which provide opportunities for understanding the physics of sunspots, wave excitation and propagation in sunspot regions, and also provide artificial data for testing the local-helioseismology inferences.

Currently, the important work of developing the synergy between the numerical simulations and local helioseismology measurements and inversions is still in an initial stage, but first important results have been obtained. This review briefly describes the current status of this effort and discusses some key problems of the local helioseismic diagnostics of sunspots.

## 2. Models of Magnetic Structures and Sunspots

The mechanism of formation of sunspots is not yet established. However, the dynamical nature of sunspots is apparent. It has been realized long ago that sunspots are a product of complex interactions of turbulent convection, radiation, and magnetic field. Cowling

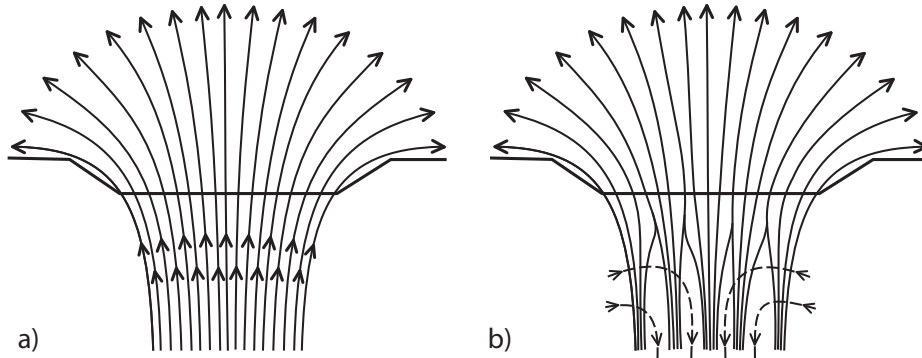


**Figure 1.** Illustrations of (a) monolithic and (b) cluster sunspot models proposed by Parker (1979). Solid curves show magnetic field lines; dashed curves show subsurface, which provide accumulation of magnetic flux and stability of sunspots.

(1946) analyzing Mt. Wilson observations of the growth and decay of sunspots first suggested that the sunspots structure cannot be magnetostatic, and that the sunspot magnetic field lines are "bunched together into the spot as a result of mass motion". Parker (1979) noticed that the formation of sunspots occurs due to coalescence of magnetic elements in regions of magnetic-flux emergence, and that the sunspot growth continues as long as "new magnetic flux (in the form of the small individual flux tubes) continues to emerge through the surface of the Sun." He argued that the subsurface structure of sunspots most likely represents loose bundles of magnetic flux tubes confined by converging downflows in the surrounding plasma beneath the solar surface (Figure 1).

In addition, theoretical investigations of magnetostatic models of sunspots (Meyer, Schmidt, and Weiss, 1977; Jahn, 1992; Moreno-Insertis and Spruit, 1989) showed that such models are intrinsically unstable, and thus dynamical effects are required for the stability of sunspots. However, theoretical modeling of the sunspot structure and dynamics, particularly of the cluster type, is a very difficult task. Therefore, magnetostatic (monolithic) models have been constructed for the purpose of comparison with spectropolarimetric observations (*e.g.* Maltby *et al.*, 1986), and more recently, for testing local helioseismology techniques (Khomenko *et al.*, 2009; Parchevsky *et al.*, 2010; Cameron *et al.*, 2010). These models play an important role for the understanding of the wave interaction with magnetic field and for helioseismology testing. However, it is important to remember that mass motions and the filamentary structure of magnetic fields are critical for the physics of both sunspots and waves propagating in sunspot regions. The magnetostatic or MHD models, in which the magnetic field lines are held together by external artificial forces (*e.g.* by setting up a boundary condition at the bottom boundary, which holds the magnetic-field concentration), cannot be considered as physically complete. Sunspots represent a self-organized dynamic phenomenon in turbulent magnetized plasma of the solar convection zone, and this is very difficult to model.

It is well known that long-lived sunspots develop penumbrae consisting of almost horizontal filamentary magnetic structures. Observations clearly show mean outflow in the penumbrae, the Evershed (1909) effect, and also a moat flow in the surrounding plasma. At first sight, these flows seem to be consistent with a diverging circulation flow pattern beneath sunspots. However, the situation may not be that simple.

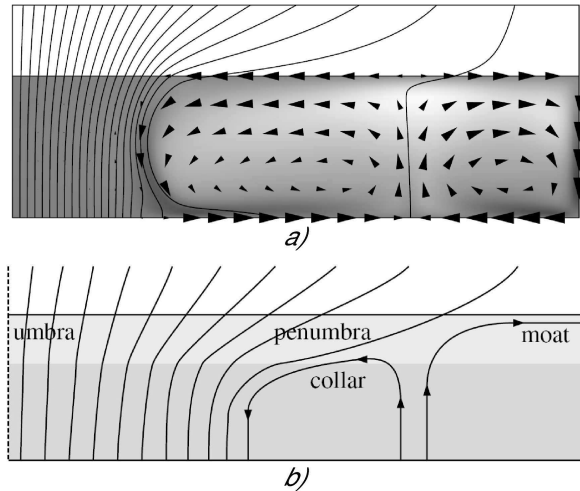


**Figure 2.** a) Flow pattern (arrows) and magnetic field lines of an axisymmetric MHD model of sunspots; b) collar and moat flows in this model (after Hurlburt and Rucklidge (2000)).

In a series of papers, Hurlburt and Rucklidge (2000), Botha, Rucklidge, and Hurlburt (2006), Botha, Rucklidge, and Hurlburt (2007), and Botha *et al.* (2008) developed numerical MHD models of the formation of magnetic structures in a convective layer and concluded that stable magnetic structures can be formed only by converging flows, and diverging flows inevitably tore the structures apart. They suggested that the Evershed and moat flows are confined in a near-surface layer, and that beneath these there is a converging “collar” flow that provides the stability of sunspots (Figure 2). The simulations of Hartlep *et al.* (2010) showed the formation of stable sunspot-like structures is accompanied by strong converging flows. The diverging flows may appear in the case of rotating sunspot structures (Figure 3), but the converging ‘collar’ flow seems to be essential for sunspot stability. These simulations were carried for axisymmetrical configurations. But, recently, Hurlburt and De Rosa (2008) confirmed in 3D simulations that large-scale magnetic structures can be formed by inflows driven by a surface cooling. However, these simulations did not reproduce the sunspot’s penumbra. Also, these simulations did not include the near-surface turbulent convection, which, in general, tends to destroy magnetic configurations.

The physics of sunspot formation, stability, and decay in the turbulent radiating plasma, and the wave excitation and propagation through this medium is very complicated. It seems that our best hope for understanding sunspots is in developing 3D MHD simulations, which take into account all essential elementary physical processes including radiative and turbulent effects. With the fast massive parallel supercomputers becoming more and more available, the solar MHD simulations are making rapid progress.

Realistic 3D MHD numerical simulations have been able to reproduce formation of relatively small pore-like magnetic structures in the turbulent upper convective layer (Stein, Bercik, and Nordlund, 2003; Vögler *et al.*, 2005; Kitiashvili *et al.*, 2010a). The simulations have shown that the concentration of magnetic field is accompanied by surface cooling and strong downdrafts and inflows around the magnetic elements (Fig-

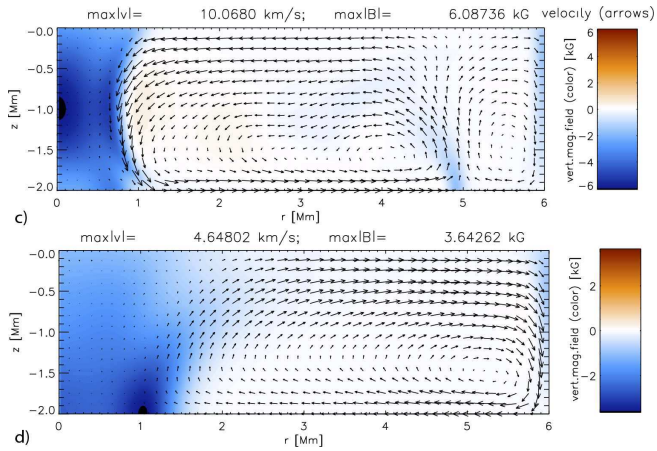


**Figure 3.** a) Simulations of axisymmetric sunspot-type structure for solar conditions with subsurface converging flow pattern; b) simulation of a rotating sunspot structure with diverging flows (Hartlep *et al.*, 2010).

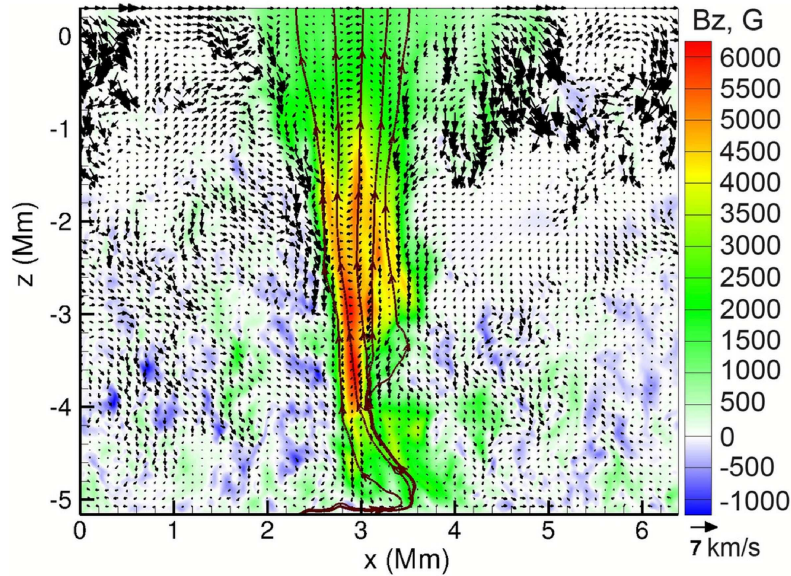


**Figure 4.** A vertical cut of the 3D MHD simulations, showing the mass flows (arrows) and the vertical magnetic field strength (background color) of a stable pore-like structure, spontaneously formed from an initially vertical magnetic field (Kitiashvili *et al.*, 2010b).

ure 4). This is consistent with the early ideas of Schmidt (1968), Ponomarenko (1972), and Parker (1979). Such converging flow pattern is also established in observations of solar pores, which do not have penumbra (Sankarasubramanian and Rimmele, 2003; Vargas Dominguez *et al.*, 2010).

The realistic MHD simulations (Heinemann *et al.*, 2007; Scharmer, Nordlund, and Heinemann, 2008; Rempel *et al.*, 2009; Kitiashvili *et al.*, 2009; Scharmer, 2009) have also led to new understanding of the sunspot penumbra structure and dynamics. The

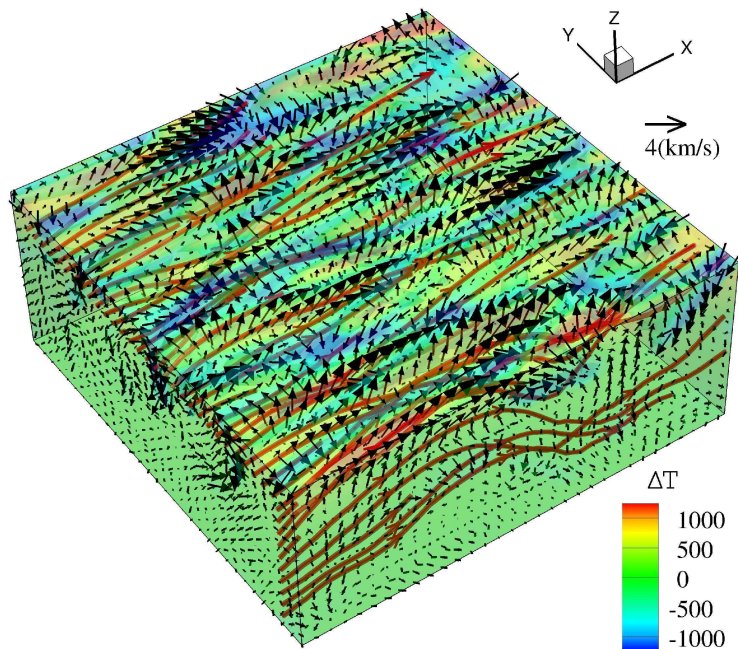


**Figure 5.** Numerical simulations of magnetoconvection in an inclined magnetic field, illustrating the origin of the Evershed flow and the filamentary structure of a sunspot penumbra. The magnetic field strength is 1000 G; the mean inclination angle is  $85^\circ$  from axis  $Z$  in the  $X - Z$ -plane. Arrows show 3D flow velocity; semi-transparent color background show the variations of temperature; red curves show magnetic-field lines. The horizontal size of the box is 6 Mm; the depth is 2 Mm (only the upper part of the 6-Mm deep simulation domain is shown) (Kitiashvili *et al.*, 2009).

simulations convincingly showed that the filamentary structure and the plasma outflow are a natural consequence of magnetoconvection in the regions of strong inclined magnetic field (Figure 5). Magnetoconvection in the inclined field has properties of waves traveling in the direction of the field inclination (Hurlburt and Rucklidge, 2000). The simulations of Kitiashvili *et al.* (2009) show that this effect contributes to the generation of the organized radial outflow in sunspot penumbrae. According to the realistic simulations the penumbra outflow (Evershed effect) represents the overturning convective motions along the magnetic field, which are also amplified and organized by the traveling magnetoconvection waves. The simulations have successfully reproduced the "sea-serpent" behavior of magnetic field lines (Sainz Dalda and Bellot Rubio, 2008; Kitiashvili *et al.*, 2010a), and showed that the Evershed flow is concentrated in the upper 1-Mm deep layer (Kitiashvili *et al.*, 2009).

The outflow outside the penumbra (called "moat flow") was first observed in Doppler velocities of the photospheric plasma (Sheeley, 1969, 1972). It is associated with an outflow of moving bipolar magnetic features (MMF). Observations also showed that the sunspot moat flow is closely related to the Evershed flow, because it is observed only on the sides of sunspots, which have the penumbrae (Sainz Dalda and Martínez Pillet, 2005; Vargas Domínguez *et al.*, 2007; Sobotka and Roudier, 2007; Vargas Domínguez

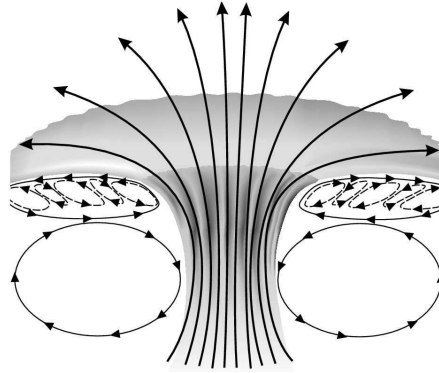


**Figure 6.** Schematic illustration of flows beneath sunspots, which shows two patterns of flow circulating in opposite directions: a shallow Evershed outflows driven by overturning convection and deeper converging flows (Zhao, Kosovichev, and Sekii, 2010b).

*et al.*, 2008; Martínez Pillet *et al.*, 2009). On the sides without penumbrae the moat flow is absent, and instead inflow is observed. Analysis of high-resolution *Hinode* data reinforced the evidence that the moat flow represents an extension of the Evershed flow beyond the penumbra boundary (Vargas Dominguez *et al.*, 2010). However, an unusual case was reported by Zuccarello *et al.* (2009) when several moving bipolar magnetic elements were observed moving away from a sunspot without penumbra. Also, observations show that the moving magnetic elements are not passively transported by the moat flow of plasma, and they can move faster than the plasma (Balthasar and Muglach, 2010). This is consistent with the sea-serpent behavior of the magnetic-field lines in the penumbra, which also produces moving bipolar elements, as was originally suggested by Harvey and Harvey (1973). The MMF flow intensifies around decaying sunspots. Thus, it is likely that it carries away some of the magnetic flux concentrated in sunspots. The moat flow has not been reproduced in simulations. Therefore, its nature is much less clear than the Evershed flow.

Radiative MHD simulations (Rempel *et al.*, 2009) have provided a fairly realistic pictures of the surface structure of sunspots. However, in subsurface layers the magnetic-field structure is held together by a boundary condition that fixes the magnetic field concentration at the bottom of the simulation domain. Once, the boundary condition is released the sunspot structure is dispersed. Unlike the stable configurations of Hurlburt and Rucklidge (2000), the subsurface flows in this model show a diverging rather than a converging pattern. This is probably the reason for the instability of the magnetic sunspot structure in Rempel's simulations.

A complete consistent model of sunspots as self-organized magnetic structures is not yet developed. However, it becomes clear that the subsurface dynamics of stable magnetic structures representing pores and sunspots must include inflows preventing a rapid dispersion of magnetic field. The Evershed and moat flows are likely to be quite shallow and driven by the overturning granular convection in the penumbra regions with almost horizontal strong magnetic field. A schematic picture of sunspot subsurface flows is given in Figure 6. The flow pattern consists of two parts: a shallow layer of overturning convection in the inclined magnetic field of penumbra, which provides the

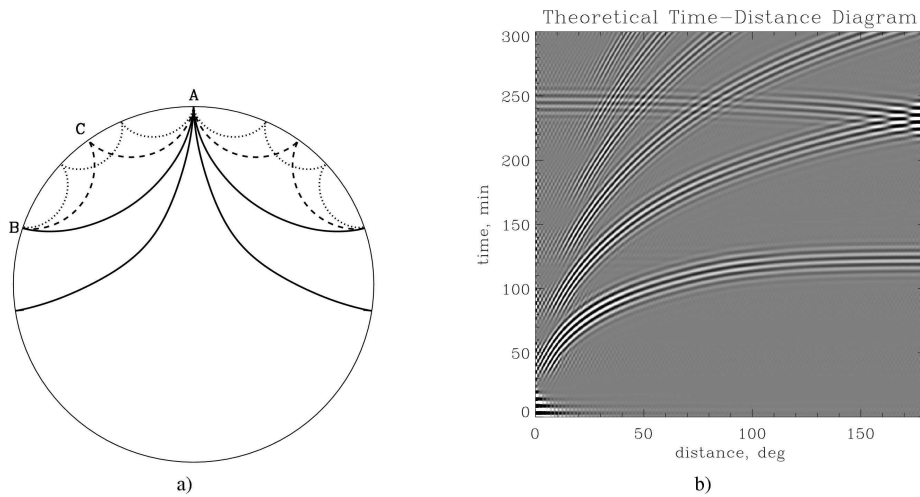


**Figure 7.** a) A sample of ray paths of acoustic waves propagating through the Sun’s interior from surface point A. b) The theoretical two-point cross-covariance of solar oscillations as a function of the distance and lag time. The lowest ridge corresponds to wave packets propagating between two points on the solar surface directly, *e.g.* along ray path AB (solid curve). The second ridge from below corresponds to acoustic waves that have an additional reflection at the surface (“second bounce”), *e.g.* along ray path ACB. This ridge appears reflected at the distance of  $180^\circ$ , because the propagation distance is measured in the interval from  $0^\circ$  to  $180^\circ$  (Kosovichev, 2003).

mean Evershed outflow, and a deeper converging (“collar”) flow beneath the Evershed flows.

### 3. Local Helioseismology Inferences of Subsurface Flows and Wave-Speed Structures

#### 3.1. Time-Distance Helioseismology

Historically, the first helioseismology inferences of the structures and flows beneath sunspots and active regions were made by using the technique of time–distance helioseismology (Duvall *et al.*, 1993). This technique is based on measuring travel times of acoustic waves. Solar acoustic waves ( $p$  modes) are excited by turbulent convection near the solar surface and travel through the interior with the speed of sound. Because the sound speed increases with depth, the waves are refracted and reappear on the surface at some distance from the source. The wave propagation paths are illustrated in Figure 7a.

The basic idea of time-distance helioseismology, or helioseismic tomography, is to measure the acoustic travel time between different points on the solar surface, and then to use these measurements for inferring variations of wave-speed perturbations and flow velocities in the interior by inversion. This idea is similar to seismology of the Earth. However, unlike in the Earth, the solar waves are generated stochastically by numerous acoustic sources in a subsurface layer of turbulent convection. Therefore, the wave travel time and other wave-propagation properties are determined from a cross-covariance function of the oscillation signals observed at different points on the solar

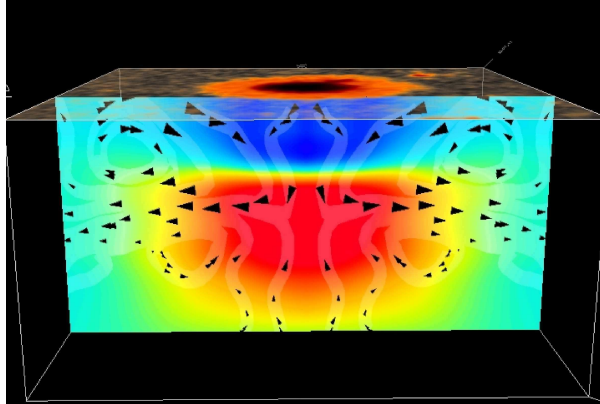


**Figure 8.** Wave-speed variations and axisymmetric component of mass flows beneath a sunspot inferred by inversion of acoustic travel times in the ray-path approximation (after Kosovichev, Duvall, and Scherrer (2000) and Zhao, Kosovichev, and Duvall (2001)).

surface. A typical cross-covariance function calculated for the whole disk is shown in Figure 7b (Kosovichev, 2003). It displays a set of ridges. The lowest ridge corresponds to wave propagating directly between two surface points, (the lowest ridge). The second ridge from below is formed by waves which experience one additional reflection at the surface on their way from point A to B, *e.g.* wavepath ACB in Figure 7a, (so-called “second bounce” ridge). The upper ridges correspond to waves with multiple reflections from the surface. The cross-covariance function represents a ‘helioseismogram’.

Duvall *et al.* (1996), using helioseismic observations from the geographical South Pole, measured the travel-time difference between the wave traveling from a sunspot and towards the spot, and they concluded that this difference could be explained by downward mass flows beneath the sunspot. Kosovichev (1996) developed a tomographic inversion procedure for the travel times, based on a ray-theoretical approximation, and obtained first subsurface maps of the sound-speed variations and flow velocities. These maps were of rather low spatial resolution ( $\approx 16$  Mm), but revealed large-scale subsurface converging flows around active regions. This technique was then improved by Kosovichev and Duvall (1997) and applied to the analysis of helioseismology data from SOHO/MDI (Kosovichev, Duvall, and Scherrer, 2000). The inversion results showed a two-layer subsurface structure of a sunspot with a negative wave-speed perturbation in the top 4–5 Mm layer and a positive perturbation in a deeper layer (Figure 8). Their results also showed the process of formation of the sunspot structure during the magnetic flux emergence. The two-layer character of the sunspot wave-speed structure has been confirmed by Jensen *et al.* (2001), Couvidat *et al.* (2004), and Couvidat, Birch, and Kosovichev (2006a), who took into account the finite-wavelength effects by using the Fresnel-zone and Born approximations. Similar inversion results were also obtained by Zharkov, Nicholas, and Thompson (2007), and most recently by Zhao, Kosovichev, and Sekii (2010b) from *Hinode/SOT* data.

These results have been a subject of debate for more than a decade mainly for three reasons: *i*) uncertainties in the travel-time measurements; *ii*) theoretical approximations used in the travel-time inversion procedures; *iii*) uncertainties in the interpretation of the inferred wave-speed perturbations in terms of the thermodynamic and magnetic

structure (because the effects of temperature and magnetic field are not separated). For instance, the travel-time measurements can be affected by errors of the Doppler-shift measurements in regions with strong magnetic field, by spatial variations of the acoustic power, and by the use of a phase-speed filter, which was applied for measuring the acoustic travel times for short distances (Duvall *et al.*, 1997).

The travel-time measurements for the short distances (0.5–2 heliographic degrees) are particularly important for inferring the shallow subsurface layer of the negative wave-speed perturbations. Qualitatively, the subsurface structure can be deduced from the travel times without inversion. Indeed, the travel-time perturbations for the short distances are positive meaning that the wave speed is reduced. For longer propagating distances, the perturbations are negative indicating faster wave propagating, and thus an increase of the wave speed.

Most of the tomographic inversions of travel-time variations have been done by using the ray-path approximation, and assuming that changes of the ray path do not significantly affect the travel-times variations (so-called Fermat’s principle) (Kosovichev and Duvall, 1997). This has been tested by using the first Born approximation, which takes into account finite wavelength and frequency effects (Birch and Kosovichev, 2000; Birch, Kosovichev, and Duvall, 2004; Couvidat, Birch, and Kosovichev, 2006b).

There have been attempts to resolve the issue of interpretation of the wave-speed inferences through modeling of the magnetostatic structure of sunspots (Olshevsky, Khomenko, and Collados, 2008; Shelyag *et al.*, 2009a; Cally, 2009). The results are obviously model-dependent, but seem to indicate that the thermal effects dominate except, perhaps, in the penumbra region, where the magnetic field is inclined. It was also noticed by Kosovichev, Duvall, and Scherrer (2000) that the interpretation of the inferred wave-speed variations purely in terms of deep magnetic fields would require a significant increase of the magnetic flux of sunspots with depth, which may be difficult to explain.

The issue of the phase-speed filtering has been investigated through modeling, which showed that because of the suppression of the acoustic power in sunspots the phase-speed filtering may result in systematic shifts in travel-time measurements (Rajaguru *et al.*, 2006). However, the systematic errors due to this effect are relatively small,  $\lesssim 10$  s (Parchevsky, Zhao, and Kosovichev, 2008; Hanasoge *et al.*, 2008), and do not affect the principal conclusions about the sunspot structure.

Using high-resolution *Hinode*/SOT observations (Kosugi *et al.*, 2007; Tsuneta *et al.*, 2008), Zhao, Kosovichev, and Sekii (2010b) have been able to measure the travel times for short distances without the phase-speed filtering procedure and confirm the positive travel-time perturbations for the acoustic waves traveling to short distances in a large-sunspot area in agreement with the results obtained with the phase-speed filtering. However, these results showed that the systematic errors may reach 20%–40%. Thus, the inferences of the wave-speed structure remain largely on a qualitative level. The uncertainties caused by the phase-filtering procedure are discussed in more detail in Section 4.3.

The tomographic inversion of acoustic travel times measured from the MDI high-resolution data revealed a converging flow pattern in the depth range of 1–5 Mm (Zhao, Kosovichev, and Duvall, 2001). This result was confirmed by analysis of *Hinode* helioseismology data (Zhao, Kosovichev, and Sekii, 2010b). The *Hinode* data have provided a more clear and convincing picture of the converging flow compared to the MDI data (Figure 9).

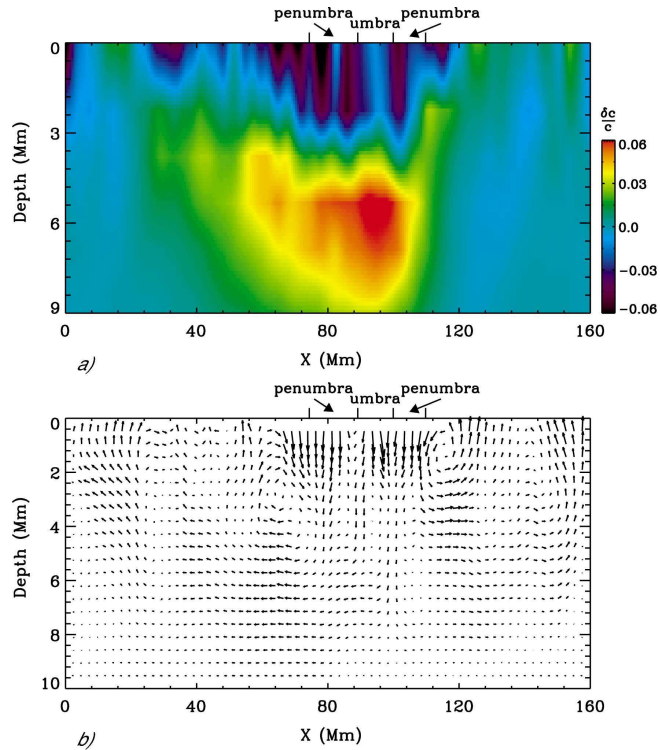


**Figure 9.** Vertical cuts through the subsurface wave-speed structure (a) and the flow field (b) of a large sunspot, obtained from the time-distance helioseismology data from *Hinode* (Zhao, Kosovichev, and Sekii, 2010b).

### 3.2. Ring-Diagram Analysis

Gough and Toomre (1983) proposed to measure oscillation frequencies of solar modes as a function of the wavevector (the dispersion relation) in local areas, and use these measurements for diagnostics of the local flows and thermodynamic properties. They noticed that subsurface variations of temperature cause change in the frequencies, and that subsurface flows result in distortion of the dispersion relation because of advection. This idea was implemented by Hill (1988) in the form of a ring-diagram analysis. The name of this technique comes from the ring appearance of the 3D dispersion relation,  $\omega = \omega(k_x, k_y)$ , in the  $(k_x, k_y)$  plane, where  $k_x$  and  $k_y$  are  $x$ - and  $y$ -components of the wave vector (Figure 10). The ridges in the vertical cuts correspond to the normal oscillation modes of different radial orders  $n$ .

The ring-diagram method has provided important results about the structure and evolution of large-scale and meridional flows and dynamics of active regions (Haber *et al.*, 2000, 2002, 2004; Howe, 2008; Komm *et al.*, 2008). In particular, large-scale patterns of subsurface flows converging around magnetic active regions were discovered Haber *et al.* (2004). These flows cause variations of the mean meridional circulation with the solar cycle (Haber *et al.*, 2002), which may affect transport of magnetic flux of decaying active regions from low latitudes to the polar regions, and thus change the duration and magnitude of the solar cycles.

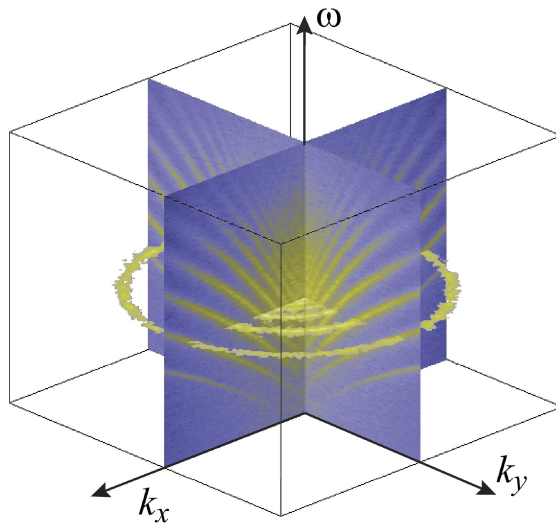


**Figure 10.** Three-dimensional power spectrum of solar oscillations,  $P(k_x, k_y, \omega)$ . The vertical panels with blue background show the mode ridge structure similar to the global oscillation spectrum. The horizontal cut with transparent background shows the ring structure of the power spectrum at a given frequency (courtesy of Amara Graps).

However, the ring-diagram technique in the present formulation has limitations in terms of the spatial and temporal resolution and the depth coverage. The local oscillation power spectra are typically calculated for regions with horizontal size covering 15 heliographic degrees ( $\approx 180$  Mm). This is significantly larger than the typical size of supergranulation and active regions ( $\approx 30$  Mm). There have been attempts to improve the resolution by doing the measurements in overlapping regions (so-called "dense-packed diagrams"). However, since such measurements are not independent, and the actual resolution is unclear. The measurements of the power spectra calculated for smaller regions (2–4 degrees in size) can increase the spatial resolution but decrease the depth coverage (Hindman, Haber, and Toomre, 2006).

### 3.3. Comparison of Local Helioseismology Results

The subsurface structure of sunspots have been inferred by three different local helioseismology techniques: time-distance helioseismology (Kosovichev, 1996; Kosovichev, Duvall, and Scherrer, 2000; Zhao, Kosovichev, and Duvall, 2001; Couvidat *et al.*, 2006c) acoustic imaging (Sun, Chou, and TON Team, 2002), and ring-diagram analysis (Basu, Antia, and Bogart, 2004; Bogart *et al.*, 2008; Gizon *et al.*, 2009). We compare these inferences for various active regions in Figure 11. In such comparison it is important to notice that the ring-diagram analysis has a substantially lower spatial and temporal resolution than the time-distance helioseismology and acoustic-imaging techniques. The spatial resolution of the time-distance inversions is typically 3–6 Mm, and the typical temporal resolution is eight hours, while for the ring-diagram analysis the typical spatial resolution is about 180 Mm, and the temporal averaging is done at least for 24 hours.

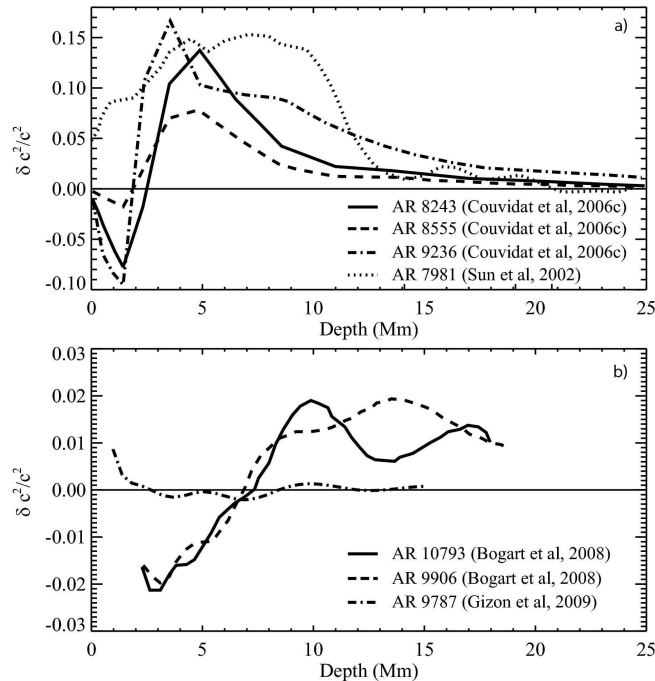


**Figure 11.** Sound-speed beneath various sunspots obtained by different local-helioseismology methods: a) time-distance helioseismology of Couvidat *et al.* (2006c) (solid, dashed and dot-dashed curves) and acoustic imaging of Sun, Chou, and TON Team (2002) (dots); b) the ring-diagram analysis of Bogart *et al.* (2008) (solid and dashed curves) and of Gizon *et al.* (2009) (dot-dashed curve).

This means that the ring-diagram results are averaged over a large area covering not only the sunspots, but the whole active region including plages and also surroundings. Thus, the ring-diagram results cannot be directly compared with the inferences for sunspots. The subsurface structure of plages is obviously different from sunspots. Also, the ring-diagram results are not simple averages of the subsurface perturbations caused by sunspots and plages, but these averages are weighted according to the acoustic-power distribution. Since the acoustic power is suppressed in sunspots and enhanced (particularly at high frequencies) in plages, it is likely that the contribution of sunspots in these inferences is smaller than this can be expected from a simple averaging. Nevertheless, it is interesting to make a qualitative comparison of the inversion results obtained by the different techniques.

We illustrate this comparison in Figure 11. The top panel shows the results of the time-distance helioseismology and acoustic imaging analyses for four sunspot regions. The sound-speed variations represent averages over the central part of sunspots relative to the surrounding quiet-Sun values. The common feature of these results is an enhancement in the deep interior 2–10 Mm, and a decrease in the subsurface layers. The time-distance results show a shallow negative variation, while the acoustic imaging inversion does not show this. The results of the ring-diagram inversions, obtained by Bogart *et al.* (2008), and also by Basu, Antia, and Bogart (2004), show the structure qualitatively similar to the time-distance results, with a positive sound-speed variation in the deep interior and a negative variation in the subsurface layer, but this layer is

deeper than in the time-distance profiles. Recently, these results were confirmed by a statistical study of Baldner *et al.* (2009), who have found the sound speed depressed in the near surface layers, but enhanced below that, and that this variations correlate with a magnetic activity index.

Surprisingly, the results published by Gizon *et al.* (2009) are drastically different from the other results obtained by the same technique. This difference could be due to an unusual structure of AR 9787, but this is unlikely because the time–distance inversions for this region according to Gizon *et al.* (2009) are similar to those shown in the top panel of Figure 11. The reasons for this difference are unclear, and currently being investigated in detail. Without such investigation it is premature to conclude that this inconsistency shows a failure of the local helioseismology inversions, as this was suggested by Gizon *et al.* (2009). Based on these results, Moradi *et al.* (2010) suggested that the sunspot in AR 9787 is most probably associated with a shallow, positive wave-speed perturbation (unlike the traditional two-layer model).

However, further investigation of the same active region (NOAA 9787) by Kosovichev *et al.* (2010) showed that the inversion results obtained by two different methods of local helioseismology, the ring-diagram analysis and time-distance helioseismology, are consistent with most of the previous results for other active regions, revealing the characteristic two-layer structure with a negative variation of the sound speed in a shallow subsurface layer and a positive variation in the deeper interior. However, there are significant quantitative differences between the inversion results obtained by the different techniques and different inversion methods. In particular, the seismic structure of the active region inferred by the ring-diagram method appears more spread with depth than the structure obtained from the time-distance technique.

It was also pointed out that the quantitative comparison of the inversion results is not straightforward because of the substantially different spatial resolutions of the helioseismology methods. The quantitative comparison must take into account differences in the sensitivity and resolution. In particular, because of the acoustic power suppression the contribution of the sunspot seismic structure to the ring-diagram signal can be substantially reduced. Kosovichev *et al.* (2010) showed that taking into account this effect reduces the difference in the depth of the sound-speed transition region. Their results obtained by the two local helioseismology methods indicate that the seismic structure of sunspots is probably rather deep, and extends to at least 20 Mm below the surface. If confirmed by further studies this conclusion has important implications for development of theoretical models of sunspots.

A systematic comparison of the subsurface flow patterns beneath sunspots and active regions has not been done. However, both, the time–distance and ring-diagram helioseismic techniques have shown remarkably similar results for large-scale subsurface flows (Hindman *et al.*, 2003, 2004), with common inflow sites around active regions as well as agreement in the general flow direction. At a depth of  $\approx 1.5$  Mm the correlation coefficient between the maps is about 0.80. As the depth increases the correlation becomes weaker. The reduction in the correlation coefficient with depth may be due to the increasing difference between the vertical resolution kernels of these techniques. Also, the recent ring-diagram inferences based on measurements of  $f$ -mode frequency shifts with a higher resolution ( $\approx 25$  Mm) revealed the near-surface outflows in the moat-flow region of sunspots (Hindman, Haber, and Toomre, 2009). This is consistent with the time–distance results also from  $f$ -mode measurements (Hindman *et al.*, 2004).

Based on the ring-diagram results, Hindman, Haber, and Toomre (2009) suggested that sunspots are surrounded by a shallow, less than 2 Mm deep, moat flows and by deeper converging large-scale flows. Because of the low resolution, the structure of the converging flows on the scale of sunspots cannot be assessed, but these inferences are not inconsistent with the time-distance results inferred from the  $f$ - and  $p$ -mode travel time measurements. Similar results in the moat flow region, obtained by a new ridge-filtering approach to time-distance helioseismology, have been reported by Gizon *et al.* (2009). However, these results indicate that the moat outflow may be extended into the deeper layers with no sign of reversed flows. The reality of such one-directional flow over a large range of depth is difficult to assess also because these measurements were based on a cross-covariance linearization method (Gizon and Birch, 2004), which may give significant systematic errors in sunspot regions, as pointed out by (Couvidat *et al.*, 2010) (Section 4.5).

Thus, in general, the theoretical picture for mature stable sunspots, illustrated in Figure 8, is consistent with the results of local helioseismology obtained by the time-distance technique (Zhao, Kosovichev, and Duvall, 2001; Zhao, Kosovichev, and Sekii, 2010b) and by the ring-diagram analysis (Haber *et al.*, 2004; Hindman, Haber, and Toomre, 2009). The measurements of the frequency shifts and travel times of the surface gravity waves ( $f$  modes) and acoustic waves ( $p$  modes) show opposite signs, consistent with an outflow in a shallow subsurface region and an inflow in the deeper interior. The surface gravity waves travel in a relatively thin subsurface layer and thus are sensitive to the properties of this layer, while the acoustic waves travel much deeper. However, these parts of the flow field beneath sunspots have been inferred by helioseismic inversions separately by inversion of the  $f$ - and  $p$ -mode travel times. An unified flow circulation pattern in sunspots has not been obtained. Developing an inversion procedure for combined  $f$ - and  $p$ -mode travel-time data is a very important task.

The current investigations also include numerical simulations of helioseismic data with flows and sunspot models for verification and testing the inferences, investigations of various uncertainties and development of new methods of local helioseismology of sunspot regions.

### 3.4. Changes of Subsurface Structures and Flows During Growth and Decay of Sunspots

The structure and dynamics of sunspots change substantially during their formation and evolution. A very important helioseismology task is to detect signature of the magnetic flux of active regions before it becomes visible on the surface and forms sunspots. However, this task turned out to be difficult because the emerging magnetic flux travels very rapidly in the upper convection zone, with a speed exceeding 1 km/s (Kosovichev, Duvall, and Scherrer, 2000). Thus, it takes less than 8 hours for the flux to emerge from the depth of 30 Mm, and the typical observing time required for measuring travel times is also eight hours. The time series for measuring frequency shifts by the ring-diagram technique are 24 hours or longer. An attempt to detect emerging flux using short two-hour time series of Doppler-shift observations of solar oscillations from SOHO/MDI was made by Kosovichev, Duvall, and Scherrer (2000). These data revealed a signature of emerging flux in the sound-speed images beneath the surface. However, no indication of emergence of a strong large-scale  $\Omega$ -loop predicted by theories has been obtained. In

addition, surface Doppler-shift observations of a large emerging active region revealed strong localized upflows and downflows at the initial phase of emergence but found no evidence for large-scale flows indicating future appearance of a large-scale magnetic structure (Kosovichev, 2009). It seems that the active regions are formed over extended period of time as a result of multiple magnetic flux emergence events. The results of time–distance helioseismology showed predominantly diverging flow patterns during the magnetic-flux emergence and decay, and mostly converging flows around stable sunspots at 1–4 Mm depth (Kosovichev and Duvall, 2006; Kosovichev, 2009). The derived vertical-flow pattern is complicated during flux emergence with intermittent up- and downflows. However, on average, the upflows are dominant at the beginning of the emergence phase, but then replaced by downflows when sunspots are developed. The flow divergence shows a correlation with flux-emergence events during the evolution of a large active region (AR 10488), but it is unclear if the flux emergence rate precedes the variation of the flow divergence or follows it.

The ring-diagram inversion results (Komm *et al.*, 2007; Komm, Howe, and Hill, 2009a,b) are generally consistent with the time–distance helioseismology inferences. The vertical velocity is not measured by this method, but estimated from the horizontal velocity pattern using a stationary continuity equation and assuming that the density stratification is horizontally uniform and corresponds to a quiet-Sun model. The accuracy of these assumptions for the case of non-stationary and non-uniform structure and dynamics of active regions has not been tested. However, these estimates show that the subsurface upflows are stronger for stronger emerging flux, and that the flows change to downflows after the active regions are developed.

## 4. Uncertainties in Local Helioseismology Inferences

### 4.1. Uncertainties of Doppler-shift Measurements

Most local-helioseismology inferences have been carried out by using solar oscillation velocity data obtained by measuring the Doppler shift of spectral lines formed in the solar photosphere. In particular, the SOHO/MDI and GONG measurements are obtained by observing the Ni I (6768 Å) line. In regions of strong magnetic field the shape of the line is affected by the Zeeman splitting and other polarization effects. In the observations the Doppler shift is calculated by averaging the left- and right circular polarized components. In the magnetic field, these components become broader because of the splitting. This results in an underestimation of the Doppler shift in the sunspot umbra when a sunspot is located in the central part of the solar disk, and in the penumbra when the sunspot is near the solar limb. The uncertainties in acoustic travel times caused by the line broadening and other radiative transfer effects in the sunspot atmosphere were investigated by Wachter, Rajaguru, and Bogart (2006a), Wachter, Schou, and Sankarabramanian (2006b), and Rajaguru *et al.* (2007), who found that around 3 mHz used for helioseismology, the systematic errors do not exceed five seconds, which is by an order of magnitude lower than the typical observed travel-time anomalies. Thus, these effects do not play significant role, but should be taken into account for improving the precision of the measurements. Wachter, Rajaguru, and Bogart (2006a) suggested a correction procedure for the Doppler-shift measurements in strong-field regions.

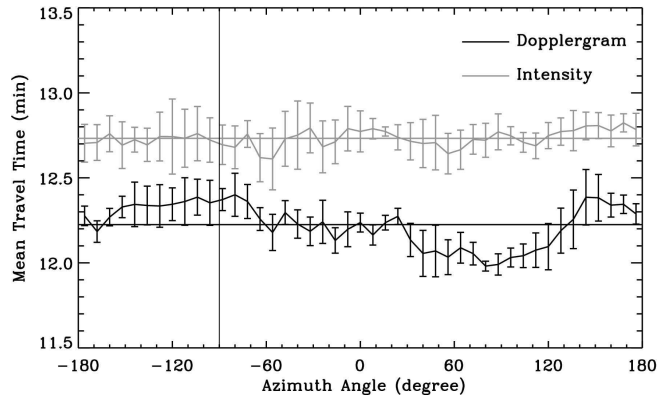


**Figure 12.** Mean acoustic travel-time variations inside a sunspot penumbra versus the azimuthal angle, measured from MDI Dopplergrams and intensitygrams for a sunspot inside AR8243 on 18-19 June 1998. The dark curve represents results computed from the Dopplergrams, and the light gray curve represents results from the continuum intensitygrams. The error bars are standard deviations. The dark and gray horizontal lines indicate the average mean travel time inside the penumbra from the Dopplergrams and intensitygrams, respectively. The vertical line indicates the azimuthal angle of the solar disk center relative to the center of the sunspot (Zhao and Kosovichev, 2006).

#### 4.2. Inclined-field (“Shower-glass”) Effect

It has been noticed by Schunker *et al.* (2005) that when a sunspot is located near the limb the phase shifts of acoustic waves (corresponding to travel times) vary in a sunspot penumbra relative to the direction to the disk center. They attributed this to a phase change of acoustic waves traveling through the inclined magnetic field of the penumbra, calling these phase perturbations “the acoustic showerglass”, and suggesting that this effect might substantially affect the inversion results.

Zhao and Kosovichev (2006) investigated this effect in detail by using the standard time–distance helioseismology procedure. They qualitatively reproduced this effect for the travel times measured from the Doppler-shift data; but found that this effect is completely absent in the travel times obtained from the MDI intensity-oscillation data (Figure 12). This means that the inclined-field effect is probably caused by the radiative transfer effects in a magnetic field, affecting the Doppler-shift measurements, rather than by changes in wave-propagation properties due to the surface magnetism. There is also a possibility that the Doppler-shift signal might be affected by changes in the relationship between the vertical and horizontal components of the oscillation in the inclined field regions. This needs to be investigated.

Since most helioseismic observations are based on Doppler-shift data, Zhao and Kosovichev (2006) investigated the systematic errors in the sound-speed inversion results caused by the inclined-field effect by comparing the inversion results for different positions of a sunspot on the solar disk. The results (Figure 13) showed that that the perturbations of the travel times cause a systematic shift of the sound-speed variations in the near-surface layers (1.5 Mm deep), but do not affect the inversion results in the deeper layers.

For the local helioseismology of sunspots, it is important that such an effect is absent in the intensity oscillation data, and that the analysis of the intensity data from

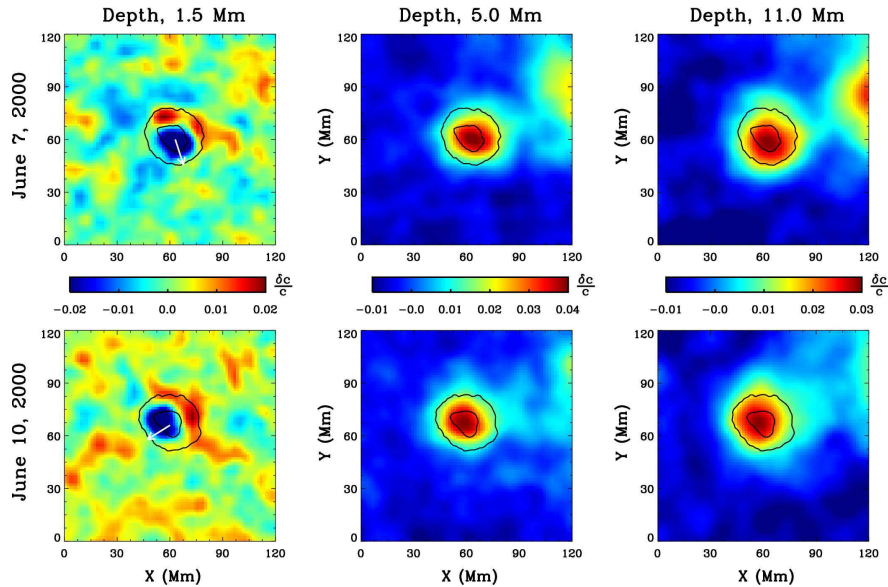


**Figure 13.** Sound-speed variations inferred from time–distance inversions for AR9026, shown at selected depths: 1.5 Mm (left), 5.0 Mm (middle), and 11.0 Mm (right), for two dates: 7 June 2000 (top) and 10 June (bottom), when the distance from the disk center was 70 and 150 degrees respectively. Contours indicate the boundaries of the sunspot umbra and penumbra determined from MDI continuum-intensity observations. White arrows at a depth of 1.5 Mm on both dates point to the solar disk center. For different dates, the image display color index is the same for the same depth, with the color bars shown in the middle row (Zhao and Kosovichev, 2006).

SOHO/MDI and *Hinode* (Figure 9) has confirmed the basic inferences obtained from the Doppler-shift data. However, for improving the precision of the local helioseismic diagnostics from Doppler-shift data it is important to develop a procedure for correcting the travel-time perturbations in the inclined-field regions of penumbrae. Also, for better understanding the physics of this effect has to be investigated by forward MHD modeling (*e.g.* Parchevsky and Kosovichev (2009)).

#### 4.3. Effects of Phase-Speed Filter and Acoustic Power Suppression

The systematic errors caused by a phase-speed filter applied to the MDI data in order to improve the signal-to-noise ratio at short travel distances are a concern (Birch *et al.*, 2009). The measurements of the acoustic travel times for short travel distances of 0.3–0.8 heliographic degrees (4–10 Mm) are necessary for inferring the structure of the shallow subsurface layers of sunspots. However, the time–distance diagrams obtained from the MDI data are corrupted by a set of horizontal ridges—artifacts, probably, due to instrumental effects and leakage of low-degree oscillations (Figure 14b–c). In the high-resolution intensity data from *Hinode* (Figure 14a), the horizontal artifact ridges are much weaker than in the MDI data. Phase-speed filtering was introduced to separate the acoustic-wave signal from the artifact in the MDI data by Duvall *et al.* (1997). The phase-speed filter is set to select the signal corresponding to the select the waves traveling to a particular range of distances using a theoretical relationship between the wave’s horizontal phase speed and the travel distance.

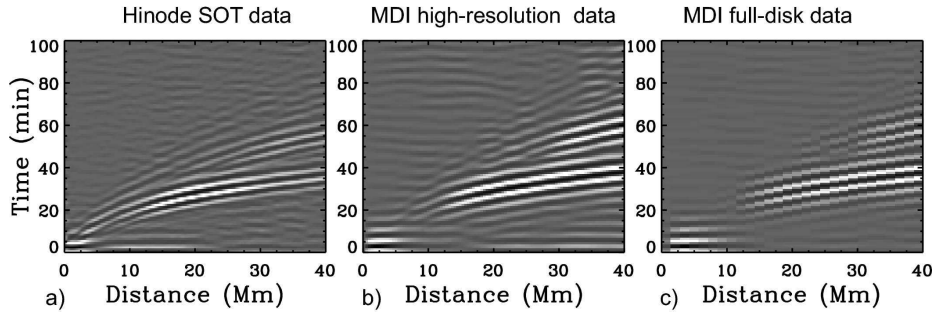


**Figure 14.** Time-distance diagrams obtained from a) *Hinode* Ca II H INTENSITY IMAGES; B) MDI HIGH-RESOLUTION DOPPLERGRAMS; C) MDI FULL-DISK DOPPLERGRAMS (KOSOVICHEV *et al.*, 2009; ZHAO, KOSOVICHEV, AND SEKII, 2010B).

Phase-speed filtering substantially improves the signal-to-noise ratio for the short-distance measurements. However, because of the strong local reduction of the oscillation power in sunspots, the phase-speed filtering causes a systematic shift in the travel times measured following the original time–distance helioseismology procedure of Kosovichev and Duvall (1997). Their formulation of the travel-time Gabor-wavelet fitting formula did not include the phase-speed filtering. Phase-speed filtering was included in the theory only recently by Nigam and Kosovichev (2010), who derived a new fitting formula. However, because of complexity, this formula has not been used. The travel-time shift in the region of acoustic-power reductions was found empirically by Rajaguru *et al.* (2006). This effect was modeled by Hanasoge *et al.* (2008) and Parchevsky, Zhao, and Kosovichev (2008), who found that the travel-time shifts are only a few seconds (reaching  $\approx 15$  seconds in an extreme case of the Hanasoge *et al.* (2008) simulations), and do not significantly change the inversion results. Generally, this effect causes underestimation of the sound-speed variations in the shallow subsurface layers. The shift can be reduced by normalizing the power variations.

Using the *Hinode* observations made with a *Solar Optical Telescope*, Zhao, Kosovichev, and Sekii (2010b) were able to obtain the travel-time measurements for short distances without phase-speed filtering and confirm the sound-speed results, obtained from the MDI data with the phase-speed filtering (Figure 15).

However, the variations of acoustic power in sunspot regions may have significant effects on inferences of subsurface flows, because the suppression of acoustic sources in sunspots causes anisotropy in wave propagation properties deduced from the cross-covariance function. This must be carefully investigated using numerical simulations.

#### 4.4. Cross-talk Effects

It is important to note that the measurements of the vertical flows by the time–distance technique may have systematic errors due to a cross-talk effect. Because of the specific geometry of the acoustic wave paths, a regular pattern of a horizontal diverging flow may give an artificial downflow contribution to the vertical-velocity estimates (Kosovichev and Duvall, 1997; Zhao and Kosovichev, 2003b). For instance, a horizontal outflow from point A in Figure 7a will accelerate the waves traveling from this point in a similar way as a downflow at this point. In some cases, when the horizontal flow

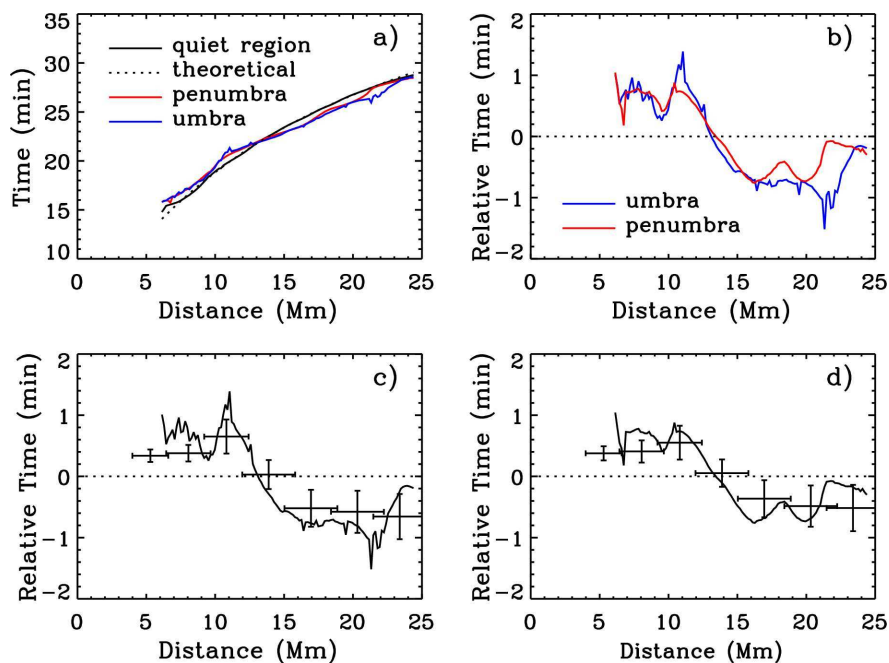


**Figure 15.** (a) Comparison of the acoustic travel times obtained for a quiet region (solid black curve), sunspot penumbra (red), and sunspot umbra (blue) without phase-speed filtering. The dotted line is an estimate from ray-path theory. (b) Travel-time differences relative to the quiet region for the sunspot penumbra and umbra without the phase-speed filtering. (c) Comparison of the travel-time differences without (curve) and with (points with errorbars) phase-speed filtering for the sunspot umbra. (d) Same as panel (c), but for the penumbra. Horizontal bars indicate the range of distances; and the vertical bars indicate the standard errors. (Zhao, Kosovichev, and Sekii, 2010b).

divergence is strong but the vertical flow is weak the inversion results for the vertical flow may give the incorrect sign. For instance, in supergranulation, where the vertical flow is very weak, the cross-talk gives an artificial downflow signal in the middle of supergranules. However, beneath the sunspots the horizontal flow is converging and the vertical flow is directed downward (Figure 8). Thus, the cross-talk effect results in an underestimation of the downflow speed, but it cannot cause a reversal in the direction of the measured vertical flows.

The role of the cross-talk effect in the travel-time inversions carried out by the LSQR method (Kosovichev and Duvall, 1997) has been studied by Zhao and Kosovichev (2003b). It has been shown that the cross-talk may be significant when the inversion results are obtained with a small number of iterations (five, - ten) in the LSQR algorithm, which is typically required for inversion of noisy data. However, the inversion with a large number of iteration ( $\approx 100$ ) substantially reduces the cross-talk and gives the correct answer even for weak vertical flows. However, this requires reducing the noise level in the travel-time measurements (*e.g.* by increasing the measurement time). For improving the diagnostics of sunspots, it is important to develop an inversion procedure specifically minimizing the cross-talk effect (Jackiewicz, 2009).

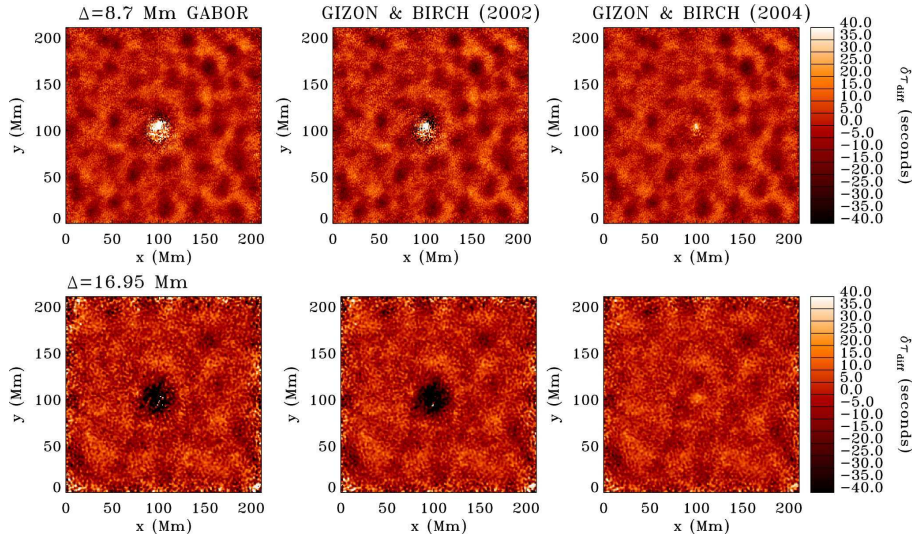


**Figure 16.** Difference travel-time perturbations for the active region NOAA 8243 obtained by using methods of fitting the Gabor wavelet (Kosovichev and Duvall, 1997) (left column), minimizing the difference between the cross-covariance functions calculated for sunspot and quiet-Sun regions (Gizon and Birch, 2002) (central column), and by linearizing this difference (Gizon and Birch, 2004) (right panel), and for two source-receiver distances (Couvidat *et al.*, 2010).

#### 4.5. Travel-time Definitions

Helioseismic travel times are measured by using the Gabor-wavelet fitting formula derived by Kosovichev and Duvall (1997). It has certain limitations because it was derived assuming the uniform distribution of acoustic sources and did not include phase-speed filtering. The phase and group travel times are measured by fitting this formula to the calculated cross-covariance function using a least-squares minimization procedure. Gizon and Birch (2002, 2004) adapted two other procedures originally developed in geophysics. The first is based on minimization in terms of least-squares of the difference between the observed cross-covariance function and a reference cross-covariance function, which can be theoretical or calculated for a quiet-Sun region. The second procedure was based on a linearization of this difference.

Recently, Couvidat *et al.* (2010) conducted extensive comparison of these procedures, and found that the travel times measured by the approaches of Kosovichev and Duvall (1997) and Gizon and Birch (2002) provide very similar results, but the linearization approach (Gizon and Birch, 2004) gives significantly different travel times (Figure 16). The reason for this discrepancy is probably in the strong variations of the acoustic power in sunspots, which are not accounted for in the linearization algorithm. In quiet-Sun regions, all three methods give consistent results. It was concluded that the use of the travel-time definition of Gizon and Birch (2004) in sunspot regions is problematic. This causes concerns about the inferences of subsurface flows reported by Gizon *et al.* (2009) based on this definition.

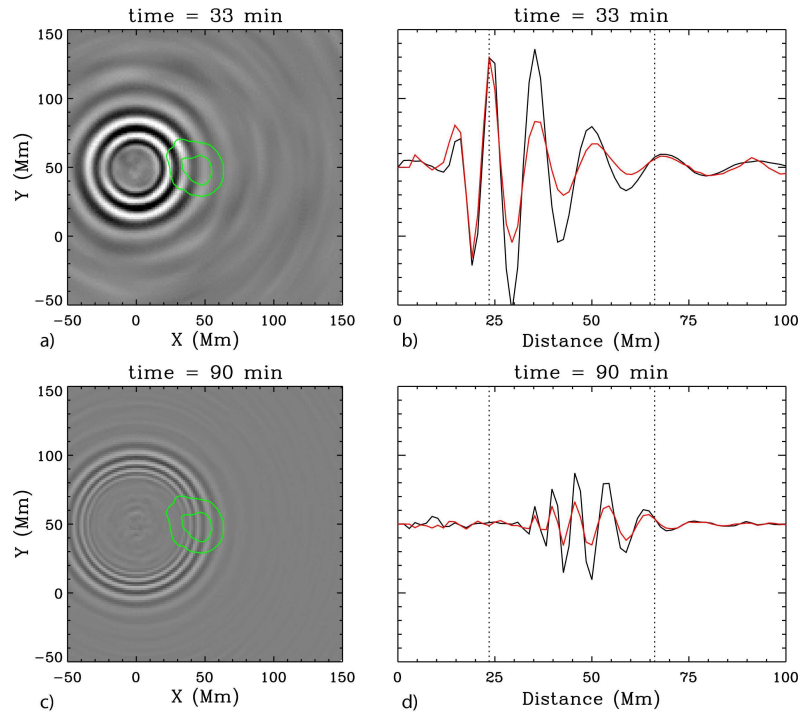


**Figure 17.** Averaged cross-correlation functions showing the interaction of acoustic ( $p$ -mode) waves (panels a) and surface-gravity waves ( $f$ -mode) waves (panels c) from an effective point source with a sunspot, at the moments when the wavefronts cross the sunspot. Panels b) and d) compare the waveforms profiles along the  $x$ -axis (red curves) with the corresponding waveforms calculated for a quiet-Sun region. The vertical lines indicate the positions of the sunspot boundaries (Zhao, Kosovichev, and Ilonidis, 2010a).

## 5. Interaction of Helioseismic Waves with Sunspots

Local helioseismic inferences are based on simple models based on basic principles of wave propagation and physical intuition. A very important role in verification and testing of these results is played by numerical 3D MHD simulations, which became possible in recent years. Substantial progress is also being made in modeling sunspots. In addition, for understanding sunspot seismology it is important to study the physics of the wave interaction with a sunspot using forward modeling. A fundamental characteristic of wave physics and seismology is the wave Green's function, which models the waves excited by elementary point sources. On the Sun such localized sources are provided by solar flares. However, in most cases the flare sources are anisotropic and moving, thus producing waves of complex shape and characteristics (Kosovichev, 2006).

In the case of stochastically excited waves, an effective Green's function is represented by the two-point cross-covariance function. With sufficient averaging in time and space this function can be visualized and compared with the results of numerical simulations of MHD waves from point sources, calculated for various sunspot models. Figure 17 illustrates the averaged cross-correlation functions for acoustic ( $p$ -mode) and surface gravity ( $f$ -mode) waves traveling through a sunspot (Zhao, Kosovichev, and

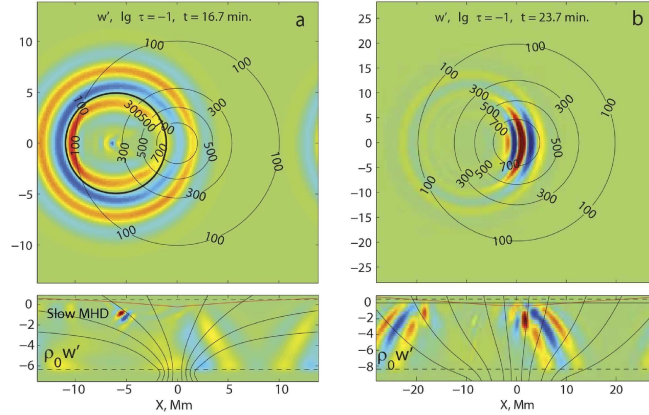


**Figure 18.** Snapshots of the vertical component of velocity of the MHD waves, excited by point sources and traveling through two sunspot models of Khomenko and Collados (2008): a) "deep" model and b) "shallow" model. Each panel consists of two pictures: nearly horizontal slice of the domain at the level  $\log \tau = -1$  (top) and the vertical cuts of the domain (bottom). Solid black curves with numbers indicating field strength represent the magnetic field lines. The black horizontal line and red curve in the vertical cuts (bottom panels) represent the position of the quiet photosphere and the level of plasma parameter  $\beta = 1$  respectively. (Parchevsky *et al.*, 2010).

Ilonidis, 2010a). These functions show how the amplitude and phase of these waves change when they travel through this spot. These changes, particularly, of the wave phase depend also on the position of the source relative to sunspot. The results show that the  $f$ -mode waves are affected by the sunspot significantly more than the  $p$ -mode waves. The  $p$ -mode waves recover their amplitude after passing through the sunspot, because they travel through the deep interior where perturbations are small, while the amplitude of  $f$ -mode waves remains reduced.

These results can be qualitatively compared with the simulations of MHD waves for two sunspots models of Khomenko and Collados (2008), obtained by Parchevsky *et al.* (2010). The simulation results (Figure 18) show that in a "deep" sunspot model the wave amplitude is reduced similar to the observations. In a "shallow" model, the amplitude is substantially increased. This is inconsistent with observations, and rules out the "shallow" sunspot model. Thus, such a forward modeling approach allows us to discriminate among sunspot models. Similar approach for an effective source extended in one direction has been recently presented by Cameron *et al.* (2010).

There is no doubt that the forward-modeling approach will be further developed and used for understanding the physics of the interaction of helioseismic waves with sunspots. The forward modeling can help in determining the relative role of magnetic and thermal effects in the wave-speed variations deduced by helioseismic inversions (Olshevsky, Khomenko, and Collados, 2008). Also, there is a potential for developing the wave-form tomography of sunspots as pointed out by Zhao, Kosovichev, and Ilonidis (2010a).

## 6. Conclusion

Local helioseismology has provided the first important insight into the subsurface structure and dynamics of sunspots that are the key elements of the Sun’s magnetic activity. A list of the initial inferences is presented in Table 1. However, because of complexity of the filamentary, turbulent and dynamic nature of sunspots there are significant uncertainties in the helioseismic inferences, which require further investigation (Table 2).

Many concerns about the local helioseismology inferences have been resolved by data analysis and numerical simulations. An important role is played by analysis of observational data from various sources.

For instance, the helioseismic observations from the *Hinode* resolved several concerns about the reliability of the MDI measurements. In particular, one concern was about the influence of the “inclined-field or magnetic shower-glass effect” (Schunker *et al.*, 2005; Schunker, Braun, and Cally, 2007), which shows that helioseismic travel times measured from Dopplergrams may depend on the line-of-sight angle in inclined magnetic fields of active regions. However, the *Hinode* results were obtained from the Ca II H intensity data, and this effect does not exist in the travel times measured from intensity oscillations (Zhao and Kosovichev, 2006). Therefore, the *Hinode* data confirmed that the previous results were not significantly affected by the inclined field “shower glass” effect. The *Hinode* data have also allowed us to qualitatively confirm the MDI time–distance helioseismology results, previously obtained with phase-speed filtering. The phase-speed filtering procedure substantially improves the signal-to-noise ratio in the travel-time measurements and will remain an essential component of this technique. Thus, it is important to take into account this procedure in the travel-time sensitivity kernels calculated using the Born approximation (Gizon and Birch, 2002; Birch, Kosovichev, and Duvall, 2004).

**Table 1.** Initial local helioseismology inferences by Time–Distance Helioseismology (TDH), Ring-Diagram Analysis (RDA), and Acoustic Imaging (AI)

Results	Method	References
Downflows under sunspots	TDH	Duvall <i>et al.</i> (1993)
Sound-speed increase beneath active regions	TDH	Kosovichev (1996)
	AI	Sun, Chou, and TON Team (2002)
	RDA	Basu, Antia, and Bogart (2004)
Sound-speed decrease in a shallow subsurface layer	TDH	Kosovichev, Duvall, and Scherrer (2000)
	RDA	Basu, Antia, and Bogart (2004)
Large-scale converging flows around AR	TDH	Kosovichev (1996)
	RDA	Haber <i>et al.</i> (2004); Komm <i>et al.</i> (2007)
Subsurface moat outflow	TDH	Gizon <i>et al.</i> (2001b)
Emerging flux and formation of AR	TDH	Kosovichev, Duvall, and Scherrer (2000); Kosovichev (2009)
	RDA	Komm <i>et al.</i> (2008)
Vortexes under rotating sunspot	TDH	Zhao and Kosovichev (2003a)
Cluster structure of a large sunspot	TDH	Zhao, Kosovichev, and Sekii (2010b)

**Table 2.** Uncertainties and tests of local helioseismology diagnostics

Uncertainties and concerns	Potential effects and solutions
Calibration of Doppler shift in strong field regions. (Wachter, Schou, and Sankarasubramanian, 2006b)	Travel-time shifts $\approx$ <i>five</i> seconds at 3 mHz. Correction procedure developed. (Wachter, Rajaguru, and Bogart, 2006a)
Phase-speed filtering and acoustic power suppression. (Rajaguru <i>et al.</i> , 2006)	Travel-time shifts up to ten seconds. Correction procedure developed (Rajaguru <i>et al.</i> , 2006). Tested by numerical simulations (Parchevsky, Zhao, and Kosovichev, 2008; Hanasoge <i>et al.</i> , 2008).
Inclined-field (“shower glass”) effect (Schunker <i>et al.</i> , 2005).	Travel-time shifts $\approx$ <i>ten</i> seconds. Absent in intensity data (Zhao and Kosovichev, 2006). Tested by numerical simulations (Parchevsky and Kosovichev, 2009).
Validity of the ray-path theory; finite-wavelength effects (Bogdan, 1997)	Tested by using a Born-approximation (Birch <i>et al.</i> , 2001; Couvidat, Birch, and Kosovichev, 2006a)
Differences in travel-time definitions: Gabor wavelet (Kosovichev and Duvall, 1997), minimization of cross-covariance deviation (Gizon and Birch, 2002), and linearization of the deviation (Gizon and Birch, 2004)	Tests using MDI data (Couvidat <i>et al.</i> , 2010) found good agreement between the travel-time definitions of Kosovichev and Duvall (1997) and Gizon and Birch (2002), but strong systematic deviations of the linearized definition of Gizon and Birch (2004).
Contributions of thermal and magnetic effects (Kosovichev and Duvall, 1997)	Tested by numerical simulations (Olshevsky, Khomenko, and Collados, 2008; Shelyag <i>et al.</i> , 2009b). Results are model dependent.
Transformation in different types of MHD waves	Studied by numerical simulations (Parchevsky and Kosovichev, 2009; Parchevsky <i>et al.</i> , 2010) and wave-form analysis of observations (Zhao, Kosovichev, and Ilonidis, 2010a). No significant effect has been found.
Relationship between surface moat outflow and deep flows	Moat outflow is observed in <i>f</i> -mode travel times (Gizon, Duvall, and Larsen, 2001a); the <i>p</i> -mode travel times correspond to deep inflows (Zhao, Kosovichev, and Duvall, 2001; Zhao, Kosovichev, and Sekii, 2010b). A unified inversion procedure for <i>f</i> - and <i>p</i> -mode has not been developed.
Cross-talk between the horizontal and vertical velocities	Studied by modeling (Zhao and Kosovichev, 2003b). It can result in underestimation of downward velocity beneath sunspots, but no artificial sign reversal. Improvement of the inversion procedure is needed (Jackiewicz, 2009).
Comparison of the time-distance and ring-diagram results	The results are in a general qualitative agreement (Hindman <i>et al.</i> , 2003, 2004; Basu, Antia, and Bogart, 2004; Bogart <i>et al.</i> , 2008). More systematic studies are needed for quantitative comparison because of the large difference in the spatial and temporal resolutions.

In addition, the important problems of local-helioseismology inversions that need to be resolved are the separation of magnetic and thermal effects, development of a unified procedure for inversion of  $f$ - and  $p$ -mode travel times, and improvement of inferences of the vertical flow component in both time–distance and ring-diagram techniques. The magnetized subsurface turbulence certainly plays a very important role in the oscillation physics, and these effects must be investigated.

Numerical simulations become increasingly important in investigations of the complicated physics of wave excitation, propagation, and interaction with magnetic regions. The synergy between the simulations and observation will allow us to improve helioseismology techniques and understanding of the sunspot structure and dynamics. The uninterrupted high-resolution helioseismology data from *Solar Dynamics Observatory* provide new opportunities for detailed investigation of the process of emergence of magnetic flux, formation, and evolution of sunspots.

## References

- Baldner, C.S., Bogart, R.S., Basu, S., Antia, H.M.: 2009, In: Dikpati M., Arentoft T., González Hernández, I, Lindsey, C. & Hill, F. (eds) *Solar-Stellar Dynamos as Revealed by Helio- and Asteroseismology: GONG 2008/SOHO 21*, Astron. Soc. Pac., San Francisco, **416**, 119.
- Balthasar, H., Muglach, K.: 2010, *Astron. Astrophys.* **511**, A67. doi:10.1051/0004-6361/200912978.
- Basu, S., Antia, H.M., Bogart, R.S.: 2004, *Astrophys. J.* **610**, 1157. doi:10.1086/421843.
- Birch, A.C., Kosovichev, A.G.: 2000, *Solar Phys.* **192**, 193.
- Birch, A.C., Kosovichev, A.G., Duvall, T.L. Jr.: 2004, *Astrophys. J.* **608**, 580. doi:10.1086/386361.
- Birch, A.C., Kosovichev, A.G., Price, G.H., Schlottmann, R.B.: 2001, *Astrophys. J. Lett.* **561**, L229. doi:10.1086/324766.
- Birch, A.C., Braun, D.C., Hanasoge, S.M., Cameron, R.: 2009, *Solar Phys.* **254**, 17. doi:10.1007/s11207-008-9282-9.
- Bogart, R.S., Basu, S., Rabello-Soares, M.C., Antia, H.M.: 2008, *Solar Phys.* **251**, 439. doi:10.1007/s11207-008-9213-9.
- Bogdan, T.J.: 1997, *Astrophys. J.* **477**, 475. doi:10.1086/303680.
- Botha, G.J.J., Rucklidge, A.M., Hurlburt, N.E.: 2006, *Mon. Not. Roy. Astron. Soc.* **369**, 1611. doi:10.1111/j.1365-2966.2006.10480.x.
- Botha, G.J.J., Rucklidge, A.M., Hurlburt, N.E.: 2007, *Astrophys. J. Lett.* **662**, L27. doi:10.1086/519079.
- Botha, G.J.J., Busse, F.H., Hurlburt, N.E., Rucklidge, A.M.: 2008, *Mon. Not. Roy. Astron. Soc.* **387**, 1445. doi:10.1111/j.1365-2966.2008.13359.x.
- Cally, P.S.: 2009, *Mon. Not. Roy. Astron. Soc.* **395**, 1309. doi:10.1111/j.1365-2966.2009.14708.x.
- Cameron, R., Gizon, L., Schunker, H., Pietarila, A.: 2010, *Solar Phys.*, in press.
- Couvidat, S., Birch, A.C., Kosovichev, A.G.: 2006, *Astrophys. J.* **640**, 516. doi:10.1086/500103.
- Couvidat, S., Birch, A.C., Kosovichev, A.G.: 2006, *Astrophys. J.* **640**, 516. doi:10.1086/500103.
- Couvidat, S., Birch, A.C., Kosovichev, A.G., Zhao, J.: 2004, *Astrophys. J.* **607**, 554. doi:10.1086/383342.

- Couvidat, S., Birch, A.C., Rajaguru, S.P., Kosovichev, A.G.: 2006, In: Bothmer V. & Hady A. A. (eds) *Solar Activity and its Magnetic Origin, IAU Symposium*, Cambridge Univ. Press, Cambridge, **233**, 75. doi:10.1017/S1743921306001499.
- Couvidat, S., Zhao, J., Birch, A.C., Kosovichev, A.G., Duvall, Jr., T.L., Parchevsky, K.V., Scherrer, P.H.: 2010, *Solar Phys.* in press.
- Cowling, T.G.: 1946, *Mon. Not. Roy. Astron. Soc.* **106**, 218.
- Duvall, T.L. Jr., Jefferies, S.M., Harvey, J.W., Pomerantz, M.A.: 1993, *Nature* **362**, 430. doi:10.1038/362430a0.
- Duvall, T.L. Jr., Kosovichev, A.G., Scherrer, P.H., Bogart, R.S., Bush, R.I., de Forest, C., Hoeksema, J.T., Schou, J., Saba, J.L.R., Tarbell, T.D., Title, A.M., Wolfson, C.J., Milford, P.N.: 1997, *Solar Phys.* **170**, 63.
- Duvall, T.L., D’Silva, S., Jefferies, S.M., Harvey, J.W., Schou, J.: 1996, *Nature* **379**, 235. doi:10.1038/379235a0.
- Evershed, J.: 1909, *Mon. Not. Roy. Astron. Soc.* **69**, 454.
- Gizon, L., Birch, A.C.: 2002, *Astrophys. J.* **571**, 966. doi:10.1086/340015.
- Gizon, L., Birch, A.C.: 2004, *Astrophys. J.* **614**, 472. doi:10.1086/423367.
- Gizon, L., Duvall, T.L. Jr., Larsen, R.M.: 2001, In: Brekke P., Fleck B., & Gurman J. B. (eds) *Recent Insights into the Physics of the Sun and Heliosphere: Highlights from SOHO and Other Space Missions, IAU Symposium 203*, Cambridge Univ. Press, Cambridge, 189.
- Gizon, L., Birch, A.C., Bush, R.I., Duvall, T.L. Jr., Kosovichev, A.G., Scherrer, P.H., Zhao, J.: 2001, In: Battrick B., Sawaya-Lacoste H., Marsch E., Martinez Pillet V., Fleck B., & Marsden R. (eds) *Solar encounter. Proceedings of the First Solar Orbiter Workshop*, SP-493, ESA, Noordwijk, 227.
- Gizon, L., Schunker, H., Baldner, C.S., Basu, S., Birch, A.C., Bogart, R.S., Braun, D.C., Cameron, R., Duvall, T.L., Hanasoge, S.M., Jackiewicz, J., Roth, M., Stahn, T., Thompson, M.J., Zharkov, S.: 2009, *Space Science Rev.* **144**, 249. doi:10.1007/s11214-008-9466-5.
- Gough, D.O., Toomre, J.: 1983, *Solar Phys.* **82**, 401.
- Haber, D.A., Hindman, B.W., Toomre, J., Bogart, R.S., Thompson, M.J., Hill, F.: 2000, *Solar Phys.* **192**, 335.
- Haber, D.A., Hindman, B.W., Toomre, J., Bogart, R.S., Larsen, R.M., Hill, F.: 2002, *Astrophys. J.* **570**, 855. doi:10.1086/339631.
- Haber, D.A., Hindman, B.W., Toomre, J., Thompson, M.J.: 2004, *Solar Phys.* **220**, 371. doi:10.1023/B:SOLA.0000031405.52911.08.

- Hanasoge, S.M., Couvidat, S., Rajaguru, S.P., Birch, A.C.: 2008, *Mon. Not. Roy. Astron. Soc.* **391**, 1931. doi:10.1111/j.1365-2966.2008.14013.x.
- Hartlep, T., Busse, F.H., Hurlburt, N.E., Kosovichev, A.G.: 2010, *ArXiv e-prints* 1006.4156.
- Harvey, K., Harvey, J.: 1973, *Solar Phys.* **28**, 61. doi:10.1007/BF00152912.
- Heinemann, T., Nordlund, Å., Scharmer, G.B., Spruit, H.C.: 2007, *Astrophys. J.* **669**, 1390. doi:10.1086/520827.
- Hill, F.: 1988, *Astrophys. J.* **333**, 996. doi:10.1086/166807.
- Hindman, B.W., Haber, D.A., Toomre, J.: 2006, *Astrophys. J.* **653**, 725. doi:10.1086/508603.
- Hindman, B.W., Haber, D.A., Toomre, J.: 2009, *Astrophys. J.* **698**, 1749. doi:10.1088/0004-637X/698/2/1749.
- Hindman, B.W., Zhao, J., Haber, D.A., Kosovichev, A.G., Toomre, J.: 2003, *Bull. Am. Astronom. Soc.*, **35**, 822.
- Hindman, B.W., Gizon, L., Duvall, T.L. Jr., Haber, D.A., Toomre, J.: 2004, *Astrophys. J.* **613**, 1253. doi:10.1086/423263.
- Howe, R.: 2008, *Adv. Space Res.* **41**, 846. doi:10.1016/j.asr.2006.12.033.
- Hurlburt, N., De Rosa, M.: 2008, *Astrophys. J. Lett.* **684**, L123. doi:10.1086/591736.
- Hurlburt, N.E., Rucklidge, A.M.: 2000, *Mon. Not. Roy. Astron. Soc.* **314**, 793. doi:10.1046/j.1365-8711.2000.03407.x.
- Jackiewicz, J.: 2009, In: Guzik J. A. & Bradley P. A. (eds) *Stellar Pulsation: Challenges for Theory and Observation*, *Am. Inst. Phys. Conf. Ser.*, **1170**, 574. doi:10.1063/1.3246565.
- Jahn, K.: 1992, In: Thomas J. H. & Weiss N. O. (eds) *Sunspots. Theory and Observations*, *Proc. NATO Adv. Res. Workshop, Cambridge, UK*, Kluwer Acad. Publ., 139.
- Jensen, J.M., Duvall, T.L. Jr., Jacobsen, B.H., Christensen-Dalsgaard, J.: 2001, *Astrophys. J. Lett.* **553**, L193. doi:10.1086/320677.
- Khomenko, E., Collados, M.: 2008, *Astrophys. J.* **689**, 1379. doi:10.1086/592681.
- Khomenko, E., Kosovichev, A., Collados, M., Parchevsky, K., Olshevsky, V.: 2009, *Astrophys. J.* **694**, 411. doi:10.1088/0004-637X/694/1/411.
- Kitiashvili, I.N., Kosovichev, A.G., Wray, A.A., Mansour, N.N.: 2009, *Astrophys. J. Lett.* **700**, L178. doi:10.1088/0004-637X/700/2/L178.

- 
- Kitiashvili, I.N., Bellot Rubio, L.R., Kosovichev, A.G., Mansour, N.N., Sainz Dalda, A., Wray, A.A.: 2010, *Astrophys. J. Lett.* **716**, L181. doi:10.1088/2041-8205/716/2/L181.
- Kitiashvili, I.N., Kosovichev, A.G., Wray, A.A., Mansour, N.N.: 2010, *Solar Phys.*, in press, *ArXiv e-prints* 1004.2288.
- Komm, R., Howe, R., Hill, F.: 2009, *Solar Phys.* **258**, 13. doi:10.1007/s11207-009-9398-6.
- Komm, R., Howe, R., Hill, F.: 2009, In: Dikpati M., Arentoft T., González Hernández, I., Lindsey, C. & Hill, F. (eds) *Solar-Stellar Dynamos as Revealed by Helio- and Asteroseismology: GONG 2008/SOHO 21*, Astron. Soc. Pacific, San Francisco, **416**, 115.
- Komm, R., Howe, R., Hill, F., Miesch, M., Haber, D., Hindman, B.: 2007, *Astrophys. J.* **667**, 571. doi:10.1086/520765.
- Komm, R., Morita, S., Howe, R., Hill, F.: 2008, *Astrophys. J.* **672**, 1254. doi:10.1086/523998.
- Kosovichev, A.G.: 1996, *Astrophys. J. Lett.* **461**, L55. doi:10.1086/309989.
- Kosovichev, A.G.: 2003, In: Thompson, M. J. and Christensen-Dalsgaard, J. (ed.) *Stellar Astrophysical Fluid Dynamics*, Cambridge Univ. Press, Cambridge, 279.
- Kosovichev, A.G.: 2006, *Solar Phys.* **238**, 1. doi:10.1007/s11207-006-0190-6.
- Kosovichev, A.G.: 2009, *Space Science Rev.* **144**, 175. doi:10.1007/s11214-009-9487-8.
- Kosovichev, A.G., Duvall, T.L.: 2006, *Space Science Rev.* **124**, 1. doi:10.1007/s11214-006-9112-z.
- Kosovichev, A.G., Duvall, T.L. Jr.: 1997, In: Pijpers F. P., Christensen-Dalsgaard J., and Rosenthal C. S. (eds) *SCORE'96 : Solar Convection and Oscillations and their Relationship*, *Astrophys. Space Science Lib.*, Kluwer Acad. Publ., **225**, 241.
- Kosovichev, A.G., Duvall, T.L. Jr., Scherrer, P.H.: 2000, *Solar Phys.* **192**, 159.
- Kosovichev, A.G., Zhao, J., Sekii, T., Nagashima, K., Mitra-Kraev, U.: 2009, In: Dikpati M., Arentoft T., González Hernández, I., Lindsey, C. & Hill, F. (eds) *Solar-Stellar Dynamos as Revealed by Helio- and Asteroseismology: GONG 2008/SOHO 21*, Astron. Soc. Pacific, San Francisco, **416**, 41.
- Kosovichev, A.G., Basu, S., Bogart, R., Duvall, T.L., Jr, Gonzalez-Hernandez, I., Haber, D., Hartlep, T., Howe, R., Komm, R., Kholikov, S., Parchevsky, K.V., Tripathy, S., and Zhao, J.: 2010, *ArXiv e-prints*, arXiv:1011.0799, *Proc. GONG 2010 - SoHO 24: A New Era of Seismology of the Sun and Solar-like Stars, J. Phys.: Conf. Ser.*, in press.

- Kosugi, T., Matsuzaki, K., Sakao, T., Shimizu, T., Sone, Y., Tachikawa, S., Hashimoto, T., Minesugi, K., Ohnishi, A., Yamada, T., Tsuneta, S., Hara, H., Ichimoto, K., Suematsu, Y., Shimojo, M., Watanabe, T., Shimada, S., Davis, J.M., Hill, L.D., Owens, J.K., Title, A.M., Culhane, J.L., Harra, L.K., Doschek, G.A., Golub, L.: 2007, *Solar Phys.* **243**, 3. doi:10.1007/s11207-007-9014-6.
- Maltby, P., Avrett, E.H., Carlsson, M., Kjeldseth-Moe, O., Kurucz, R.L., Loeser, R.: 1986, *Astrophys. J.* **306**, 284. doi:10.1086/164342.
- Martínez Pillet, V., Katsukawa, Y., Puschmann, K.G., Ruiz Cobo, B.: 2009, *Astrophys. J. Lett.* **701**, L79. doi:10.1088/0004-637X/701/2/L79.
- Meyer, F., Schmidt, H.U., Weiss, N.O.: 1977, *Mon. Not. Roy. Astron. Soc.* **179**, 741.
- Moradi, H., Baldner, C., Birch, A.C., Braun, D.C., Cameron, R.H., Duvall, T.L., Gizon, L., Haber, D., Hanasoge, S.M., Hindman, B.W., Jackiewicz, J., Khomenko, E., Komm, R., Rajaguru, P., Rempel, M., Roth, M., Schlichenmaier, R., Schunker, H., Spruit, H.C., Strassmeier, K.G., Thompson, M.J., and Zharkov, S.: 2010, *Solar Phys.* **267**, 1.
- Moreno-Insertis, F., Spruit, H.C.: 1989, *Astrophys. J.* **342**, 1158. doi:10.1086/167673.
- Nigam, R., Kosovichev, A.G.: 2010, *Astrophys. J.* **708**, 1475. doi:10.1088/0004-637X/708/2/1475.
- Olshevsky, V., Khomenko, E., Collados, M.: 2008, *12th European Solar Physics Meeting*, <http://espm.kis.uni-freiburg.de/>, p.3.2.
- Parchevsky, K.V., Kosovichev, A.G.: 2009, *Astrophys. J.* **694**, 573. doi:10.1088/0004-637X/694/1/573.
- Parchevsky, K.V., Zhao, J., Kosovichev, A.G.: 2008, *Astrophys. J.* **678**, 1498. doi:10.1086/533495.
- Parchevsky, K., Kosovichev, A., Khomenko, E., Olshevsky, V., Collados, M.: 2010, *ArXiv e-prints* **1002.1117**.
- Parker, E.N.: 1979, *Astrophys. J.* **230**, 905. doi:10.1086/157150.
- Ponomarenko, Y.B.: 1972, *Soviet Astron.* **16**, 116.
- Rajaguru, S.P., Birch, A.C., Duvall, T.L. Jr., Thompson, M.J., Zhao, J.: 2006, *Astrophys. J.* **646**, 543. doi:10.1086/504705.
- Rajaguru, S.P., Sankarasubramanian, K., Wachter, R., Scherrer, P.H.: 2007, *Astrophys. J. Lett.* **654**, L175. doi:10.1086/511266.
- Rempel, M., Schüssler, M., Cameron, R.H., Knölker, M.: 2009, *Science* **325**, 171. doi:10.1126/science.1173798.

- Sainz Dalda, A., Bellot Rubio, L.R.: 2008, *Astron. Astrophys.* **481**, L21. doi:10.1051/0004-6361:20079115.
- Sainz Dalda, A., Martínez Pillet, V.: 2005, *Astrophys. J.* **632**, 1176. doi:10.1086/433168.
- Sankarasubramanian, K., Rimmele, T.: 2003, *Astrophys. J.* **598**, 689. doi:10.1086/378883.
- Scharmer, G.B.: 2009, *Space Science Rev.* **144**, 229. doi:10.1007/s11214-008-9483-4.
- Scharmer, G.B., Nordlund, Å., Heinemann, T.: 2008, *Astrophys. J. Lett.* **677**, L149. doi:10.1086/587982.
- Schmidt, H.U.: 1968, In: Kiepenheuer K. O. (ed.) *Structure and Development of Solar Active Regions, IAU Symposium*, D. Reidel, Dordrecht, **35**, 95.
- Schunker, H., Braun, D.C., Cally, P.S.: 2007, *Astron. Nach.* **328**, 292. doi:10.1002/asna.200610732.
- Schunker, H., Braun, D.C., Cally, P.S., Lindsey, C.: 2005, *Astrophys. J. Lett.* **621**, L149. doi:10.1086/429290.
- Sheeley, N.R. Jr.: 1969, *Solar Phys.* **9**, 347. doi:10.1007/BF02391657.
- Sheeley, N.R. Jr.: 1972, *Solar Phys.* **25**, 98. doi:10.1007/BF00155747.
- Shelyag, S., Zharkov, S., Fedun, V., Erdélyi, R., Thompson, M.J.: 2009, *Astron. Astrophys.* **501**, 735. doi:10.1051/0004-6361/200911709.
- Shelyag, S., Zharkov, S., Fedun, V., Erdélyi, R., Thompson, M.J.: 2009, In: Dikpati M., Arentoft T., González Hernández, I., Lindsey, C. & Hill, F. (eds) *Solar-Stellar Dynamics as Revealed by Helio- and Asteroseismology: GONG 2008/SOHO 21*, Astron. Soc. Pacific, San Francisco, **416**, 167.
- Sobotka, M., Roudier, T.: 2007, *Astron. Astrophys.* **472**, 277. doi:10.1051/0004-6361:20077552.
- Stein, R.F., Bercik, D., Nordlund, Å.: 2003, In: Pevtsov A. A. and Uitenbroek H. (ed.) *Current Theoretical Models and Future High Resolution Solar Observations: Preparing for ATST*, Astron. Soc. Pacific, San Francisco **286**, 121.
- Sun, M., Chou, D., The TON Team: 2002, *Solar Phys.* **209**, 5. doi:10.1023/A:1020909524039.
- Tsuneta, S., Ichimoto, K., Katsukawa, Y., Nagata, S., Otsubo, M., Shimizu, T., Suematsu, Y., Nakagiri, M., Noguchi, M., Tarbell, T., Title, A., Shine, R., Rosenberg, W., Hoffmann, C., Jurcevich, B., Kushner, G., Levay, M., Lites, B., Elmore, D., Matsushita, T., Kawaguchi, N., Saito, H., Mikami, I., Hill, L.D., Owens, J.K.: 2008, *Solar Phys.* **249**, 167. doi:10.1007/s11207-008-9174-z.

- Vargas Domínguez, S., Bonet, J.A., Martínez Pillet, V., Katsukawa, Y., Kitakoshi, Y., Rouppe van der Voort, L.: 2007, *Astrophys. J. Lett.* **660**, L165. doi:10.1086/518123.
- Vargas Domínguez, S., Rouppe van der Voort, L., Bonet, J.A., Martínez Pillet, V., Van Noort, M., Katsukawa, Y.: 2008, *Astrophys. J.* **679**, 900. doi:10.1086/587139.
- Vargas Dominguez, S., de Vicente, A., Bonet, J.A., Martinez Pillet, V.: 2010, *A&A* **516**, A91.
- Vögler, A., Shelyag, S., Schüssler, M., Cattaneo, F., Emonet, T., Linde, T.: 2005, *Astron. Astrophys.* **429**, 335. doi:10.1051/0004-6361:20041507.
- Wachter, R., Rajaguru, S.P., Bogart, R.S.: 2006, In: *Proceedings of SOHO 18/GONG 2006/HELAS I, Beyond the spherical Sun*, SP-624, ESA, Noordwijk, p.48.1.
- Wachter, R., Schou, J., Sankarasubramanian, K.: 2006, *Astrophys. J.* **648**, 1256. doi:10.1086/505930.
- Zhao, J., Kosovichev, A.G.: 2003, *Astrophys. J.* **591**, 446. doi:10.1086/375343.
- Zhao, J., Kosovichev, A.G.: 2003, In: Sawaya-Lacoste, H. (ed.) *GONG+ 2002. Local and Global Helioseismology: the Present and Future*, SP-517, ESA, Noordwijk, 417
- Zhao, J., Kosovichev, A.G.: 2006, *Astrophys. J.* **643**, 1317. doi:10.1086/503248.
- Zhao, J., Kosovichev, A.G., Duvall, T.L. Jr.: 2001, *Astrophys. J.* **557**, 384. doi:10.1086/321491.
- Zhao, J., Kosovichev, A.G., Ilonidis, S.: 2010, *Solar Phys.* in press.
- Zhao, J., Kosovichev, A.G., Sekii, T.: 2010, *Astrophys. J.* **708**, 304. doi:10.1088/0004-637X/708/1/304.
- Zharkov, S., Nicholas, C.J., Thompson, M.J.: 2007, *Astron. Nach.* **328**, 240. doi:10.1002/asna.200610744.
- Zuccarello, F., Romano, P., Guglielmino, S.L., Centrone, M., Criscuoli, S., Ermolli, I., Berrilli, F., Del Moro, D.: 2009, *Astron. Astrophys.* **500**, L5. doi:10.1051/0004-6361/200912277.

